Marine Pollution Bulletin 191 (2023) 114979

Contents lists available at ScienceDirect

Marine Pollution Bulletin

journal homepage: www.elsevier.com/locate/marpolbul

An impact-based environmental risk assessment model toolbox for offshore produced water discharges

Raymond Nepstad [a,*], Konstantinos Kotzakoulakis [a], Bjørn Henrik Hansen [a], Tor Nordam [a,b], JoLynn Carroll [c]

[a] SINTEF Ocean, Trondheim, Norway
[b] Department of Physics, NTNU, Trondheim, Norway
[c] Akvaplan-niva, Tromsø, Norway

ARTICLE INFO

Keywords:
Produced water
Environmental risk assessment model
Toxicokinetics
Toxicodynamics
Individual-based model

ABSTRACT

We present a novel approach to environmental risk assessment of produced water discharges based on explicit impact and probability, using a combination of transport, fate and toxicokinetic-toxicodynamic models within a super-individual framework, with a probabilistic element obtained from ensemble simulations. Our approach is motivated by a need for location and species specific tools which also accounts for the dynamic nature of exposure and uptake of produced water components in the sea.

Our approach is based on the well-established fate model DREAM, and accounts for time-variable exposure, considers body burden and effects for specific species and stressors, and assesses the probability of impact. Using a produced water discharge in the Barents Sea, with early life stages of spawning haddock, we demonstrate that it is possible to conduct a model-based risk assessment that highlights the effect of natural variations in environmental conditions. The benefits, limitations and potential for further improvements are discussed.

1. Introduction

In the process of extracting crude oil from sub-sea hydrocarbon reservoirs, water may constitute a fraction of the liquid phase. This *produced water* (PW) is a combination of formation water and injected water which contains a highly complex mixture of dispersed crude oil, aromatic hydrocarbons, alkylphenols, ketones, heavy metals, dissolved gases, suspended particles, salts, organic acids, added production chemicals and naturally occurring radioactive materials (Lee and Neff, 2011). For offshore operations, PW is either injected back into the formation or treated to meet regulatory limits and then discharged into the surrounding ocean. PW is among the largest intentional industrial discharge to the worldwide marine environment, with annual discharges in the North-Atlantic (OSPAR) area of 300 $\times$ 10^6 m^3, containing 4000 tons of crude oil (Beyer et al., 2020; OSPAR, 2019).

Despite only accounting for a small fraction of the total PW discharge, dispersed oil and polycyclic aromatic hydrocarbons (PAHs) are considered non-negligible risk components of PW (Beyer et al., 2020; Rye et al., 1998), and some risk calculations have shown a contribution between 15 % (Smit et al., 2011) and 20 % (Ditlevsen, 2017) to the total risk. Most PAHs are considered persistent, bioaccumulative and toxic, and offshore monitoring programs have repeatedly demonstrated PAH uptake in caged mussels and fish as well as wild-caught fish (Brooks et al., 2011), however, indications of environmental impact are minor (Hylland et al., 2008). A recent review summarised the current status of knowledge regarding environmental effects of PW discharges on the Norwegian Continental Shelf (NCS) (Beyer et al., 2020). Among the key knowledge gaps highlighted was the unknown potential of PW discharges, containing small amounts of crude oil and dissolved PAHs, to cause toxicity to sensitive early life stages of pelagic-spawning fish, with subsequent unknown consequences for population recruitment in important spawning areas. Also highlighted were the repeated findings of elevated DNA adduct concentrations in wild-caught haddock (*Melanogrammus aeglefinus*). Increased DNA adduct concentrations have not been found in caged fish placed close to PW sources in the North Sea (Brooks et al., 2011). Nevertheless, the observed increased concentrations in haddock has led to DNA adducts being a priority biomarker for exposure to hazardous PAH exposure (Beyer et al., 2020).

The environmental risk of PW discharges can be assessed in different ways but generally follows a tiered approach (IOGP, 2020). If lower tiers

* Corresponding author.
E-mail address: raymond.nepstad@sintef.no (R. Nepstad).

https://doi.org/10.1016/j.marpolbul.2023.114979
Received 21 December 2022; Received in revised form 18 April 2023; Accepted 19 April 2023
Available online 29 April 2023

indicate high risk, additional data is obtained and a more detailed assessment is made at the next tier. Different "lines of evidence" may be used to assess risk in this context, e.g., determining risk of adverse effects to a set of test species at different levels of dilution of the raw PW. The levels thus obtained can then be compared with predicted dilution for the actual PW effluent, which can be calculated with numerical models. In this approach, also known as whole effluent toxicity (WET), a specific distance is defined beyond which concentrations from the discharge are required to be below established effect levels (IOGP, 2020; Karman and Smit, 2019). This method is relatively simple to apply, and has the advantage of including potential toxic effects from the whole PW, both known and unknown constituents. However, WET does not provide information on which components in the PW that are driving the risk.

If the risk is found to be high, WET does not provide the information needed to take actions to reduce the risk, as may be required. The information about which component is driving the risk may be found by substance-based approaches, where chemically quantified components in the PW are tested for toxicity. Following the European Chemical Agency (ECHA) (ECHA, 2008), predicted environmental concentration (PEC) is compared with its predicted no-effect concentration (PNEC). This is the basis for the generic OSPAR Risk-Based Approach (RBA) (Ospar, 2012), applied for individual substances chemically quantified or measured in the PW, which is used in the Environmental Impact Factor (EIF) (Johnsen et al., 2000; Reed and Rye, 2011). The EIF is calculated from dynamic model-predicted PEC of each component, by comparison to pre-established PNECs (Reed and Rye, 2011). Components that contribute the most to the EIF can then be targeted for reduction or substitution, thus reducing the overall environmental risk of the PW discharge, and this approach has been successfully used to bring risk down over time on the NCS (Smit et al., 2011). In a recent study the WET and substance-based approaches for several PW sources in the OSPAR area were compared (De Vries et al., 2022). The substance-based approach were found to either under- or overestimate toxicity in some cases, due to incorrect discharge concentrations of known components or the presence of unknown components in the PW. For the WET approach, it was pointed out that when limited acute toxicity testing was used it would not capture chronic effects over longer time scales. Therefore, it was recommended that both approaches be applied regularly and their predictions compared. We note, however, that both approaches are fundamentally limited by the PNEC being a threshold for continuous exposure, while in reality exposure will vary in time, with uptake and depuration rates determining the internal concentration in an organism. For additional discussion of the relative strengths and weaknesses of WET and substance-based approaches, see, e.g., IOGP (2020, p. 17).

While existing approaches to PW environmental risk assessment (ERA) such as EIF and WET are useful for screening whether discharges exceed a predetermined effect threshold (or not), they cannot generally be used to determine the site-specific environmental impact, because they do not account for the dynamic exposure to local populations of marine species, nor include specific toxicity thresholds and processes for these species. There are however some examples were site-specific assessments has been used, such as the ERA study addressing the possible effect of offshore PW alkylphenols (APs) on reproduction in North Sea fish populations (Beyer et al., 2012). Through the use of toxicokinetic-toxicodynamic (TKTD) models, species- and exposure-specific predictions of toxic effects can be made (Jager et al., 2011). We have here developed a numerical tool which integrates TKTD models with a super-individual-based model (sIBM) approach (Grimm and Railsback, 2005; Nepstad et al., 2021; North et al., 2009; Scheffer et al., 1995) to the representation of marine species. Specifically the General Unified Threshold model of Survival (GUTS) have been chosen, a widely used framework (see e.g., Bart et al., 2021; Cedergreen et al., 2017; Jager and Ashauer, 2018; Jager et al., 2017; Sardi et al., 2019), which the European Food Safety Authority (EFSA) considers ready for ERA use in certain cases (E. P. on Plant Protection Products et al., 2018). By further coupling the TKTD module with a well-established transport-fate model for PW (DREAM (Nepstad et al., 2022a; Reed and Hetland, 2002; Reed and Rye, 2011)), the necessary components for predicting effects from one or more PW components on a specific species are in place. Finally, an ensemble simulations (Nordam et al., 2016; World Meteorological Organization, 2012) approach within DREAM provides the means to sample seasonal and inter-annual variability in environmental conditions. This allows us to calculate the probability of different impact outcomes, which is used here as an explicit element in the risk calculation.

The new modelling and risk assessment capabilities described in this paper are generic, but in order to apply it to a specific location additional input data is required, such as spatial distribution of a locally relevant species, and basic biological trait of that species (e.g., weight and lipid content). We note that a similar approach, incorporating TKTD and super-individual-based models, has recently been applied for assessing population and ecosystems impacts of acute oil spills (Carroll et al., 2022; Carroll et al., 2018).

In this paper, we present the basis and assumptions for the new model, and we demonstrate its use and predictions with a theoretical PW discharge scenario in the Barents Sea. We discuss how the present approach constitutes a useful extension of the PW environmental risk toolbox, as well as some of its limitations.

2. Method

The model consists of several linked modules handling different aspects: PW transport and fate, super-individual representation and transport, TKTD and ensemble simulations. Most of the mathematical descriptions are referenced from the literature, and a summary is given in the Supplementary information.

PW discharged to the sea will undergo dilution, through transport and mixing by ocean currents, and degradation processes including biodegradation by bacteria. In DREAM these processes are encapsulated in the transport-fate model component, based on a Lagrangian particle formulation (Nepstad et al., 2022a; Reed and Hetland, 2002; Reed and Rye, 2011). PW transport is calculated by solving the Lagrangian transport equation (van Sebille et al., 2018), with offline forcing provided through 3D currents and 2D wind fields (network Common Data Form, netCDF input). In addition to dilution due to transport and mixing, bacterial degradation of PW components can occur in the oceanic environment, with a range of different half-lives (Lofthus et al., 2018). This is handled by a first-order kinetics approach in the model, based on measured degradation rates for each PW component and Q_{10}-adjusted to the local sea temperature (Bagi et al., 2013). We use a factor of 2 for the Q_{10}-coefficient, which means that rates double on each 10 °C increase in temperature above the reference (13 °C), and are similarly halved below this reference. Depending on the situation, primary (removal of initial component) or ultimate (total breakdown to water and CO_2) biodegradation rates may be used in a model scenario. Concentrations for each PW component is calculated on a 3D grid from the masses and positions tracked by each Lagrangian particle, with higher-resolution grids near the discharge source(s) to better resolve the initial concentrations. The model has previously been used to predict PW transport and concentrations in connection with a field study of PW discharges on the Scotian Shelf outside Canada, and proved valuable when interpreting measurements from the field (Niu et al., 2016). Reasonable agreement with measured dilution and plume location was found, although there were limitations in detecting the main core of plume with the experiment design (Niu et al., 2016).

The spatio-temporal predictions of PW component concentrations are used to further predict impacts on marine organisms, through coupling with a super-individual model (North et al., 2009; Scheffer et al., 1995). In this approach, individual organisms are represented as Lagrangian particles with specific properties and behaviours intended to capture key aspects of their physical counterparts. Properties include

weight, growth rate and lipid fractions, while behaviours include diurnal vertical migration and buoyancy, which in part determine positions in the water column and thus influence exposure to PW components. Consecutive life stages with different properties can be configured in the model, so that a super-individual may for example be tracked from egg to larva, if a fish early life stage (ELS) is studied.

External time- and position-dependent concentrations are translated to internal concentrations (dose) in each super-individual using a one-compartment toxicokinetic (TK) model. Effects are predicted from this internal dose with either the GUTS-IT (Individual Tolerance) or GUTS-SD (Stochastic Death) toxicodynamic (TD) models (Jager et al., 2011; Jager and Ashauer, 2018).

In the GUTS-IT variant, each super-individual has its own tolerance, drawn from some distribution. Effects are incurred immediately, and are a function of the maximal dose experienced by that super-individual during the simulation (i.e., effect cannot decrease with time). 50 % effect occurs when the dose reaches the individual tolerance level. This variant is broadly similar to the Critical Body Residue approach (see e.g., McCarty and Mackay, 1993; Meador et al., 2011).

The GUTS-SD variant has a different approach, where effects are accumulated dynamically once an internal no-effect concentration (NEC) is reached. Effect accumulation proceeds at a rate proportional to how much the internal concentration exceeds the threshold, multiplied by a rate factor called the killing rate. The TKTD module implemented here builds on earlier published work (Nepstad et al., 2021). Mathematical details can be found in the Supplementary information.

2.1. Parameters in the TKTD model

GUTS models use a set of parameters that can be obtained by fitting to experimental survival data. Procedures and recommendations for this approach are detailed in Jager and Ashauer (2018), and there are several recent studies which use this approach (Bart et al., 2021; Cedergreen et al., 2017; Gergs et al., 2016; Sardi et al., 2019). While fitting GUTS to data is the ideal approach that generally provides the optimal model parameter values as well as corresponding uncertainty distributions, it relies on time-resolved laboratory data for the species and components in question, which are rarely available for the multitude of relevant PW components and local species of interest. More often only acute LC50 values based on short-term exposure and some basic chemical descriptors are available. To overcome this issue we use QSARs to assess model parameters for a given species and chemical components, based on individual (e.g., weight, lipid fraction) and chemical (e.g., k_{ow}) properties. Such relationships have been previously reported for GUTS-SD (Baas et al., 2015), and while less accurate than specific data, can nevertheless be useful. The flow from input values via specific QSARs to model parameters is illustrated in Fig. 1.

Uptake and elimination rates for the one-compartment toxicokinetic model are obtained with the Optimal Modeling for Ecotoxicological Applications (OMEGA) model (De Hoop et al., 2013; Hendriks et al., 2001), based on super-individual weights and lipid fractions, combined with k_{ow} for each PW component, in the same manner as previously reported (Nepstad et al., 2021). The median internal individual effect threshold, m_i, for component i, is obtained from the LC50 value of that component, using the equilibrium solution of the one-compartment model:

$$m_i = \mathrm{LC50}_i \times P_{iw}/ACR. \quad (1)$$

Here, P_{iw} is the partition coefficient from external to internal concentration (bio-concentration factor), obtained from the OMEGA model. An acute-to-chronic ratio, ACR, is applied to obtain chronic survival threshold, where a value of 10 can be used as a first approximation for non-polar narcotic chemicals (Hiki and Iwasaki, 2020). The distribution of internal tolerances used by GUTS-IT is by default log-normal, and uses a width-parameter of 5 (see Eq. (25) and Table 1 in the Supplementary information) (Smit et al., 2011). The $\mathrm{LC50}_i$ values can be specified as input on a per-component level, or as a log-linear relationship from k_{ow}.

For the GUTS-SD model, which has two parameters in the toxicodynamic part, the no-effect (internal) concentration (NEC, z_i) is set at the 5-percentile of the GUTS-IT distribution median (m_i), while the killing rate b_i follows a k_{ow}-based regression,

$$\log b_i = a \log k_{ow} + b. \quad (2)$$

Values for the coefficients a, b may be found in e.g., Baas et al. (2015). Variation in NEC among different species for a model hydrocarbon was studied by Sardi et al. (2019).

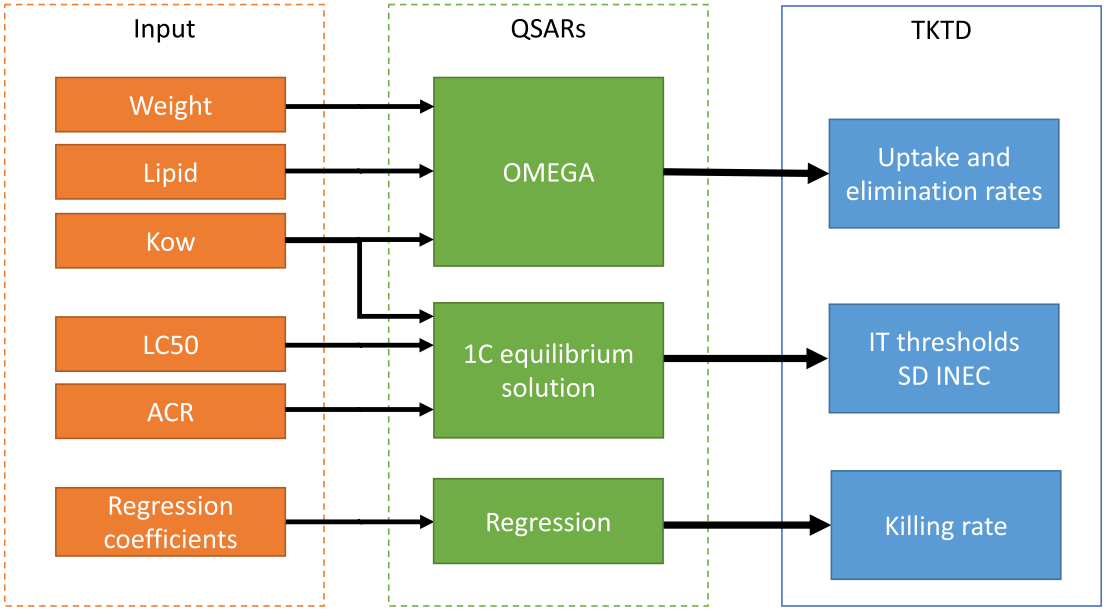

Fig. 1. Sketch of toxicokinetic-toxicodynamic (TKTD) model inputs and Quantitative Structure-Activity Relationships (QSARs) used in the parameter prediction layer. User-specified parameters on the left, such as weight, lipid fraction, LC50 and acute-to-chronic ratios (ACRs) are used in the QSAR layer to predict TKTD model parameter values. The underlying mathematical details of this scheme can be found in the Supplementary information (Sections 1.3–1.4 and Table 1). See also manuscript text for further details, and the acronym list towards the end of the manuscript.

2.2. Ensemble simulations and risk

In ERA risk (R) should be based on probability (P) and impact (I) (i.e. $R = P \times I$) (Jager, 2016). Impacts can be derived from TKTD modelling, while probability can be determined by multiple model runs based on a range of possible input variables.

In environmental risk assessment for oil spills, Monte Carlo simulations are used to assess the distribution of possible outcomes (see e.g., Liubartseva et al., 2021; Nordam et al., 2016; Nordam et al., 2017). Here, we propose adapting the same approach for PW risk assessment. Natural variability in environmental conditions influences the transport and fate of PW between years and seasons. We sample from this variability to create a distribution of potential outcomes through the use of ensemble simulations. Specifically, we obtain a large archive of environmental data (ocean currents, wind, temperature, salinity, etc.), ideally spanning several years. We then sample from different model simulation start dates, which in turn samples the environmental conditions. For each start date, we run a simulation of the same base scenarios, where each simulation is called an ensemble member. Endpoints, such as biological impact, from each ensemble member are then combined to calculate an environmental risk index based on statistics from the ensemble as a whole.

In each ensemble member, the transport-fate model and the TKTD model are combined to calculate a measure of impact, which can for example be the fraction of non-surviving individuals. For a given species, each numerical super-individual, i, represents a number n_i of physical individuals of that species, and k_i is the fraction of dead individuals in that super-individual, at the end of the simulation. The total fraction of non-surviving individuals in a simulation is then given by $K = \sum_i n_i k_i / \sum_i n_i$, where the sums are over all super-individuals representing the species of interest.

Considering the whole ensemble of simulations, we can calculate the risk as the product of impact and probability. We let K_j be the fraction of non-surviving individuals in ensemble member j. Using the fraction of dead individuals as our measure of impact, we calculate the risk index as

$$R = \sum_{j=1}^{N} P_j K_j, \tag{3}$$

where P_j is the probability of simulation j occurring, and N is the number of simulations in the ensemble. Assuming equal probability for each simulation, the risk index simplifies to

$$R = \frac{1}{N} \sum_{j=1}^{N} K_j. \tag{4}$$

We note that it is possible to include several different species in each simulation, each with their own specific behaviours and TKTD parameters, which means that we can calculate a risk index for several different species from the same ensemble.

3. Model demonstration simulations

The Johan Castberg oil field (referred to as Castberg in this text) is located in the south-west part of the Barents Sea, around 210 km south of Bear Island. In the immediate area around Castberg, the water depth varies between 360 m and 400 m. In the vicinity of Castberg there are known occurrences of Haddock (*Melanogrammus aeglefinus*), a species that typically spawns in March–April (Bogstad et al., 2013), and we focus on early life stages of this species in our simulations. Sea temperatures vary throughout the year, but in March (haddock spawning) typically the upper parts of the water column are well-mixed and not stratified. According to World Ocean Atlas climatology (Locarnini et al., 2018), the March mean sea temperature is approximately 4.7 °C throughout the upper water column around Castberg. Mean sea surface temperatures (WOA) and mean current directions (from the Nordic 4 ocean model (Lien et al., 2013)) for March 2019 are shown in Fig. 2, and these are also used as model input forcing. The prevailing current direction is generally towards the east around Castberg, and we thus expect a PW discharge to drift towards the east.

3.1. Produced water scenario at Castberg

Developed by Equinor and originally scheduled to begin operation in 2022, the Castberg facility will rely on re-injection of PW back into the reservoir, and is thus not planning to have PW discharges to the ocean (Dahl-Hansen et al., 2017). However, down-time on the re-injection system or other unforeseen events may lead to PW discharges to the ocean for limited periods of time. Several scenarios for PW discharge during such downtime have been investigated in the public environmental risk assessment report for Castberg (Dahl-Hansen et al., 2017), and these have varying probability and potential impact. For our simulations we will consider one of these scenarios, named "Scenario 0" in the ERA report. This is an alternative scenario intended to contrast how an operational situation without any re-injection and 100 % discharge of PW to sea would look. Although not a realistic scenario, it can be expected to give the highest impact compared to the other scenarios defined in the report (Dahl-Hansen et al., 2017). These other discharge scenarios with lower discharge volumes will result in lower exposure concentrations, internal concentrations and effect levels. We note that our simulations here are intended only as an illustration case for the new model tool.

PW from Castberg in the scenario considered here ("Scenario 0") is discharged from 20 m depth (position 20.262997 E, 72.504201 N) at a discharge rate of 20,815 m^3/day, which is the prognosis rate for 2030 (Dahl-Hansen et al., 2017). We include 26 naturally occurring organic oil component groups in the simulated discharge, while inorganic components such as metals and production chemicals have not been included. The key properties and discharge concentrations of the included components are tabulated in the Supplementary information (Tables 2 and 3).

3.2. sIBM model setup for Haddock early life stages

There are known spawning grounds for Haddock located west and south of Castberg, stretching up from Lofoten along the coast, as shown in Fig. 2. The potential impact from PW discharges on ELS from this spawning ground has been the focus in this case study.

The continuous PW discharge starts 9 days before the Haddock spawning, which is set up to last from 1st to 31st March, and the total simulation duration is 60 days. The positively buoyant egg stage duration, adjusted for mean sea temperatures, is set to 20 days, followed by a 20 day planktonic larval stage, and finally by a second larval stage with an eastward swimming tendency (10 mm/s or 36 m/h). While swimming behaviour can be found in older larvae, here it is simply intended as a demonstration of this model feature, and not based on specific data. A summary of parameter values for this part of the model setup can be found in Table 1.

We used 40,000 Lagrangian particles to represent the PW in this simulation, where 100 were released per model time step. The model time step was set to 10 min, and model output from the model calculations was stored every 2 h. A supporting grid of 2000 m × 2000 m × 10 m was used to calculate PW concentrations from the Lagrangian particles, with a higher resolution grid at 150 m × 150 m × 8 m was used in a 22 km square centred on the discharge point. Haddock ELS was represented using 30,000 super-individual particles.

3.3. Uptake and effect model input

When available, LC50 values for individual components and specific species can be used directly as model input. These data are then used by the model to calculate the GUTS threshold parameters (see Section 2.1).

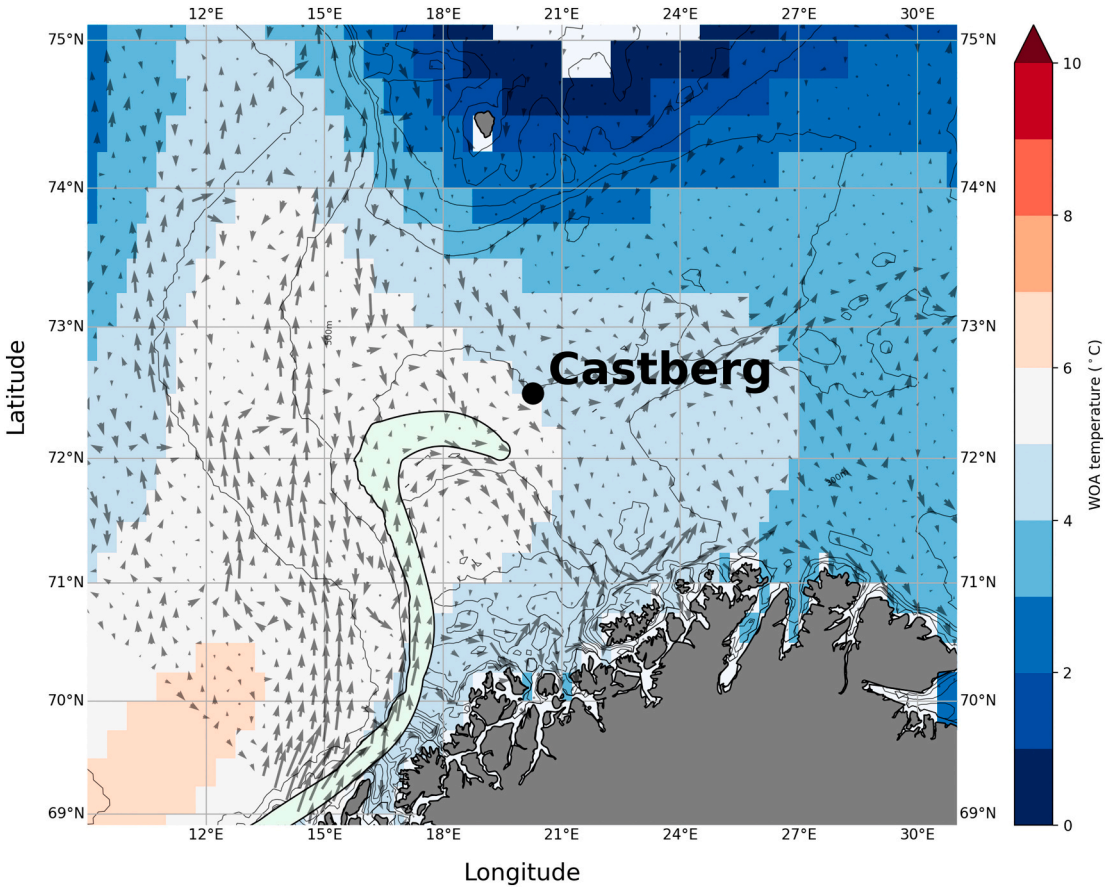

Fig. 2. Mean sea surface temperature (World Ocean Atlas) and mean current directions for March 2019 according to the Nordic4 ocean model, with longer arrows indicating higher current speeds. The location of Castberg is indicated by the black marker, while nearby spawning grounds for Haddock is indicated by the shaded green area with black outline. (For interpretation of the references to color in this figure legend, the reader is referred to the web version of this article.)

Table 1
Input parameters for the sIBM model, for Haddock ELS. See text for details, and Supplementary information for the underlying equations.

Parameter	Unit	Egg stage	Larvae 1	Larvae 2
Lipid fraction	m^3/m^3	0.02	0.05	0.05
Initial length	mm	1.5	–	–
Shape factor	–	3	3	3
Length-weight parameter	kg/m^n	536	536	536
Growth rate	mm/day	0	0.1	0.1
Buoyancy	–	Positive	Neutral	Neutral
Swim speed	mm/s	0	0	10

The lack of specific data for Haddock ELS for all the PW components considered here requires the use of QSARs, which the model also supports, in the form of a k_{ow}-based regression for LC50s. Many options for such regressions exist in the literature (see e.g., Di Toro et al., 2007; EU, 2003; French-McCay, 2002), but some literature values reported in Dahl-Hansen et al. (2017) suggest slightly lower LC50 values than the published regressions. Here we used a regression based on back-calculating from a fixed internal threshold value (m_i^j) of 0.5 mmol/kg for each component, using the equilibrium solution for the one-compartment model and P_{iw} values for Haddock eggs (full green line in Fig. 3). See Eqs. (12) and (24) in the Supplementary information for further details. This is slightly more conservative than the range for acute non-polar narcosis of 2–8 mmol/kg commonly reported in the

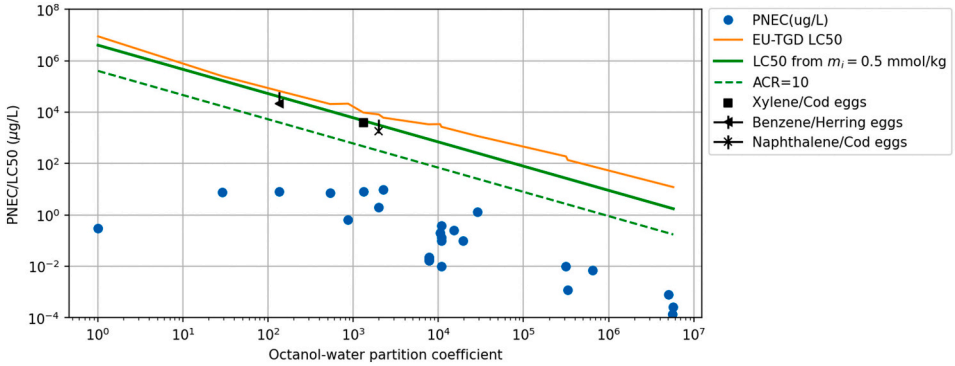

Fig. 3. Different options for LC50 values as a function of k_{ow}, in units of µg/L. PNEC values taken from Ditlevsen (2017) and OSPAR (2014) are shown for comparison (blue round markers indicate the individual components considered here). Measured LC50 values for specific components (black markers) are taken from Table 4.11 in Dahl-Hansen et al. (2017). The EU Technical Guidance Document (TGD) LC50 line is defined in the Supplementary information (Eq. (26)). See text for discussions and more details. (For interpretation of the references to color in this figure legend, the reader is referred to the web version of this article.)

literature (e.g., Meador et al., 2011), but yields values which are close to reported literature LC50s for certain single components (see Fig. 3). We further use an acute-to-chronic ratio (ACR) of 10 (Hiki and Iwasaki, 2020; McGrath and Di Toro, 2009), and the resulting LC50/ACR values are also shown in Fig. 3 (dashed green line). The resulting GUTS threshold values are shown in Fig. 4 (lower right panel), as a function of k_{ow}.

For elimination rate and partition coefficient, the OMEGA model is used with lipid and weight parameters for each stage (Table 1). These depend on the k_{ow} of each component, as illustrated in Fig. 4 (upper row panels). The values are tabulated in the Supplementary information (Table 3).

3.4. Total internal concentrations and effects

The summary of predictions of population exposure, total internal concentrations (sum of all components in discharge) and effects are shown in Fig. 5. We see that while around 30 % of the population is exposed to the PW from Castberg[1] (dashed line in panel B), the maximum and population 99-percentile total internal concentrations[2] are low (orange and green dashed line in panels C and D), less than 35 ng/g and 0.45 ng/g respectively. The predicted population effect using GUTS-IT (chronic mortality, using an acute-to-chronic ratio of 10, see above) is essentially zero, indicated by the blue line in panel A of Fig. 5 (less than 0.014 per billion). Simulations with GUTS-SD results in numerically zero effect, due to the NEC never being reached by any super-individual in the simulation (results not shown). This result must be interpreted in the context and limitations here, where we only consider a subset of discharge components (only naturally occurring organic oil components). The environmental risk assessment for Castberg (Dahl-Hansen et al., 2017) concluded that population-level effects on plankton and fish were likely to be negligible.

Trajectories of the 20 super-individuals with the highest total internal concentration are shown in Fig. 6. The majority of these appear to be originating from the part of the spawning ground (green shaded area) closest to Castberg (orange circle), while two originate further west and south. From inspection of the internal concentrations of these super-individuals, we determine that the main contributing components are BTEXs, napthalenes and phenanthrenes, with some traces of phenols. The BTEX are among the most volatile components, with the shortest biodegration half-lives in the input data used here, and exposure to these is most likely to occur close to the discharge, which is consistent with the trajectories of the top super-individuals (Fig. 6).

3.5. Component internal concentrations

The model also allows us to inspect in detail the exposure and internal concentration history of each super-individual in the simulation. This data was used to correlate internal concentrations with distance from the discharge. For this analysis, we focused on a few components which are prominent in the total internal concentration (Section 3.4), and which cover a range of k_{ow} values: toluene, naphthalenes, phenanthrenes and phenol. Model results for the super-individuals with the highest and 10th highest total internal concentrations (measured by maximal value across the duration of the simulation) are shown in Fig. 7 (upper and lower set of figures, respectively). The map figures on the left show the individual trajectories of the super-individuals, with Castberg marked by the orange circle, and the corresponding depth of the super-individuals are shown in the inset axis. The top super-individual passes within 1.1 km of Castberg, while the 10th one gets to 200 m at the closest, in general both having an eastward transport trend in addition to tidal motion. The distance from Castberg at any time can be found in the lowermost panel on the right-hand side for each super-particle row (vertical axis labelled "Dist. from Castberg (km)"). From the component internal concentrations time series shown in the panels to the right in Fig. 7, we see that each super-individual essentially have elevated exposure and internal concentrations only very near in time to their closest pass by the discharge point (marked by a vertical dashed red line in the right-hand panels of Fig. 7). This happens during the egg stage for the top super-individual, but in the larval stage for the 10th one.

3.6. Ensemble simulations

Here we run a small ensemble of 32 simulations, using "Scenario 0" from the previous section, varying the start year between 2017 and 2020, and the start date between 1 and 15 March (spawning timing is also adjusted to match). In this case, the variable forcing included currents (Nordic4) and winds (ERA5). A summary of results of the ensemble simulations is shown in Fig. 8, specifically the distributions of population-mean chronic mortality (%). The results are grouped by simulation start year, and the variability of each box in the box plots originates from variable start date (between 1 and 15 March) within that year. We observe that the population mean chronic mortality is overall very small (near 0) for all simulations, consistent with the results from the previous section, and the calculated risk index was 10^{-7} %. There is some variation between years, and also within each year, with the highest values occurring for the 2020 simulations.

4. Discussion

The ability to predict location- and species-specific impacts and risks from PW is a very useful addition to the environmental impact assessment toolbox. In a recent review of PW discharges fate and effects in the Norwegian offshore sector, Beyer et al. recommended that both toxicokinetic and toxicodynamic factors be considered when extrapolating from laboratory data to field conditions, in the process of determining environmental risk (Beyer et al., 2020). The present model tool offers a step forward in this regard compared to existing tools based on whole-effluent or substance-based PEC/PNEC approaches, as illustrated with the case study in the previous section. Data for locally relevant species, together with the required ocean data such as currents, are combined with the mechanistic approach to provide more insight into the actual exposure and effect. Naturally, there will be more variability in the output results from such an approach, but this reflects a variability that exists in nature, and that is now being accounted for to a larger extent. At the same time, more effort, both human and computational, is required to set up and run such location- and species-specific models, and they do come with increased complexity. This can make them harder to understand, and results more difficult to interpret and explain. Designing an adequately accurate scenario for the area of interest and obtaining relevant input data of a high enough quality both remain challenging. Nevertheless, when used appropriately, we believe there are tangible benefits to the presented approach.

Another aspect of location-specific mechanistic models is that they allow for reduction in the conservatism in underlying assumptions and input. Instead of generic PNECs, species-specific thresholds and parameters can be used, and direct dynamic exposure, uptake and effects on individuals replace volume of influence (risk) concepts. However, some conservatism still remains, for instance in the use of acute-to-chronic ratios, but this is not an inherent limitation in the model, but necessitated by the lack of data at present. Several studies have pointed to the need for experiments designed to provide the needed data to parameterise mechanistic TKTD models (Jager et al., 2017; Sardi et al., 2019). If such data were available they would immediately enhance the value and accuracy of our model approach.

While the effect predictions from the new DREAM model extension have not been compared to measurements, several of its parts are based

[1] Defined as the relative number of super-individuals having a total internal concentration above 1e-5 ng/g at any point during the simulation.

[2] Both of these are calculated with respect to all active super-individuals.

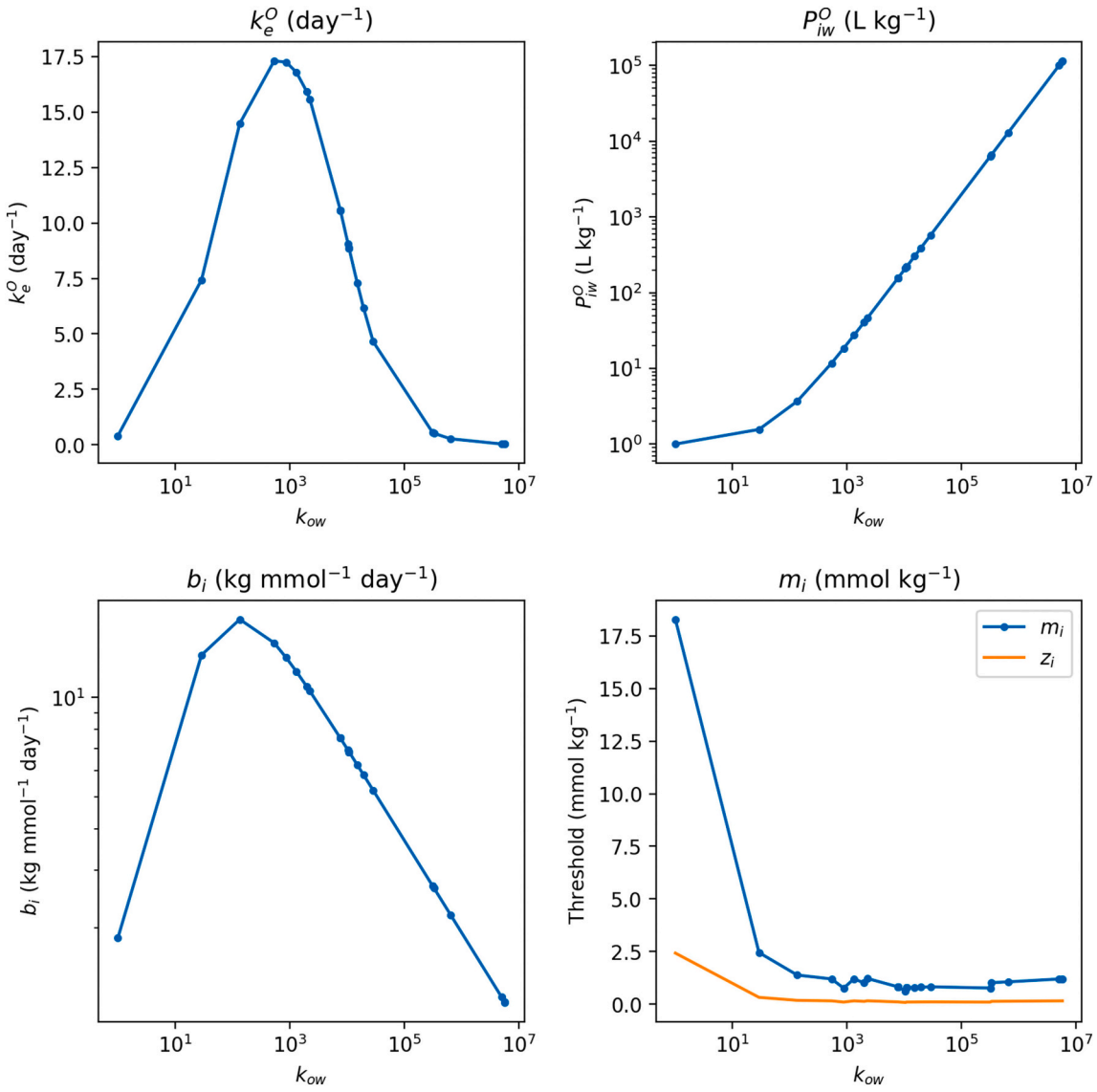

Fig. 4. GUTS parameter values for the Haddock egg stage used in the simulations. Upper left panel: TK elimination rate k_e^O. Upper right panel: partition coefficient (bioconcentration factor) P_{iw}^O. Lower left panel: Killing rate b_i. Lower right panel: GUTS-IT threshold m_i and GUTS-SD NEC z_i.

on established and separately tested components (e.g., GUTS). Moreover, the fate component in DREAM has been corroborated by comparison with field measurements in several previous studies (Durell et al., 2006; Niu et al., 2016). Through the Norwegian biannual water column monitoring (WCM) programme (Brooks et al., 2011), which investigates effects from oil and gas activities on the NCS, a recently conducted monitoring campaign at the Ekofisk installation in the North Sea has provided direct measurements of both PW plume dilution and internal concentration in blue mussels. Comparison between these data and model predictions showed reasonable agreement (Nepstad et al., 2022b).

Generally, it is difficult to isolate population-level impacts from a specific anthropogenic discharge, such as PW, in the marine environment. Obtaining population estimates from sampling requires long-term regional campaigns, and cumulative impact from multiple stressors to these populations also needs to be considered. The modelling approach taken in this work can be used to assess one complex chemical mixture stressor (PW) as part of a multi-stressor environment causing cumulative effects. As such it can be used to assist spatial analysis to predict overlapping threats and better understand contribution and possible interactions between multiple stressors. To compare model predictions to real-world scenarios, controlled placement of fish and mussel cages at increasing distances from a PW discharge (Brooks et al., 2011) may offer the best compromise. However, uncertainties still remain when extrapolating such results to wild and free-moving individuals in the water column (Beyer et al., 2020).

From the demonstration simulations presented in Section 3, it is clear that super-individuals passing near the discharge points exhibit the highest internal concentrations. These receive the highest exposure concentrations, which are generally transient, and levels correlate with proximity to the discharge. In principle a super-individual could be trapped in an eddy and return to the discharge area, in which case a second pulse of exposure could be experienced. We did not observe this in the present simulations for the super-individuals with highest internal concentration, however, trajectory crossings further from the discharge were observed (Fig. 6). This, combined with the dynamic and short-lived nature of the (highest) exposure pulses underscores the importance of toxicokinetics when assessing effects. We note that this is different from typical experimental situations, where longer exposure durations at constant levels are commonly used.

In addition to organic oil components such as PAHs, PW may contain production chemicals, organic acids and metals (Beyer et al., 2020).

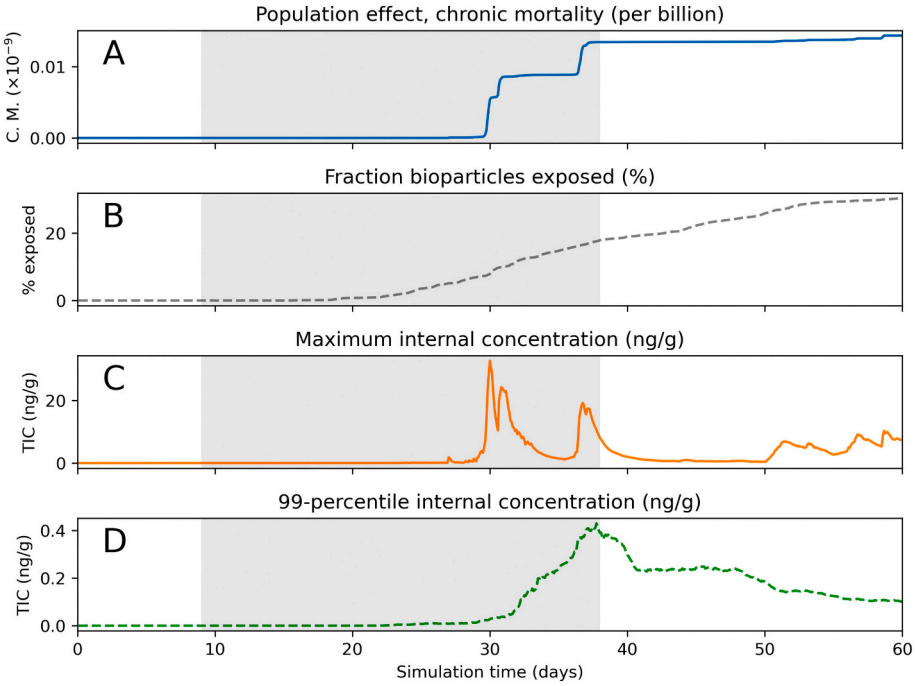

Fig. 5. Panel A: population chronic mortality (blue full line). Panel B: relative number of exposed super-individuals (black dashed line). Panel C: population-maximum total internal concentration (orange full line). Panel D: population 99-percentile total internal concentration (green dashed line). The grey shaded area indicates the duration of spawning. The total internal concentrations are sum over all components. See text for discussion. (For interpretation of the references to color in this figure legend, the reader is referred to the web version of this article.)

While the present model approach is well suited for organic oil components and production chemicals, it is more limited when it comes to metals, which tend to have specific modes of action, and for which whole body residue (internal concentration) approaches have limited utility (Adams et al., 2011). While fate and exposure may be studied with the model, effect predictions for PW mixtures including metals are beyond its present scope. However, a recent study was able to successfully parameterise a GUTS model on survival data for heavy metals binary mixture exposure (Bart et al., 2021), pointing towards possible future extensions of the model. Another remaining challenge is the inclusion of biotransformation, internal enzymatic processes (e.g., cytochrome P450 1a (CYP1A) in fish), which in most cases reduces the toxicity and increases excretion of PAHs. When comparing internal PAH concentration predictions from simulations to those measured in environmentally exposed fish, which have high biotransformation capacity, their rate of PAH biotransformation will be a confounding factor. Biotransformation can also result in more harmful metabolites being formed, as has been shown for benzo[*a*]pyrene (Baird et al., 2005). This, along with more-than-additive toxicity shown for some PAH-mixtures and PAH-metal mixtures (Gauthier et al., 2014) may potentially affect precision of the toxicity estimations. For equally or less harmful metabolites resulting from such processes, a modified elimination rate could in principle be used, but would require specific data for the species and compound in question, which is typically not available.

The ensemble simulation presented in Section 3.6 is conducted in order to show an example of the natural variability in impact. In an actual application, the number of ensemble members would be larger, and the environmental data archive would ideally span a longer period. The risk index, *R*, can be calculated as given by Eq. (3), but other statistics from the full ensemble are also useful. As defined here, the risk index is essentially the expectation value of impact, but for some skewed distributions, other statistics such as the median or 90-percentile may help illustrate the range of possible outcomes. The use of ensemble simulations allows us to calculate these statistics, which would not be available from a single simulation.

The risk index may be of most use in situations where changes to upstream conditions are studied, expressed through multiple different model scenarios where the discharge rate or composition is changed, for instance. Then the relative changes in the risk between scenarios are of more interest than its absolute value, and can be used to rank scenarios from most to least favourable from an environmental perspective. This is not unlike how the EIF is used today, where simulations with different discharge profiles are compared to find lower risk options (lower EIF value), but based on a more comprehensive model accounting for site-specific biological impact and risk.

5. Conclusion and outlook

We have developed a new numerical model tool for impact and risk assessment of PW discharges into the marine environment. The model combines a well-established fate model (DREAM) with an impact model based on super-individuals and TKTD, and an ensemble simulation module for finding probabilities. Using model parameters describing relevant species, and spatio-temporal distribution of that species, we find locally relevant environmental impact. Sampling from an archive of data for site-specific environmental conditions (temperature, wind, currents, etc.), we can find probabilities of different impacts. By combining impact and probability, we make it possible to truly address questions of risk from PW releases in a rigorous manner.

The new model tool has been demonstrated for a PW discharge case in the Barents Sea with early life stages of Haddock spawning in the area. An ensemble simulation was conducted, where the variation between ensemble members highlights the effect natural variations in environmental conditions can have on the impact. With the new model, it is thus now possible to conduct a model-based risk assessment that includes, and also goes beyond, what the IOGP recommends for Tier 2: Locally relevant data are taken into account, along with physico-chemical marine processes, and the dynamical nature of the plume of discharged PW (IOGP, 2020, p. 29). In addition we can consider the variability between years, and address probabilities of different impacts.

Future applications at different sites can provide more specific insights into environmental risk drivers from PW discharges. Ongoing work in comparing internal concentration data from field sampled copepods and blue mussels will provide information about the precision of body burden estimations. Future acquisition of species-specific data on toxicokinetics and acute/chronic toxicity thresholds will obviously improve the precision of the simulation output.

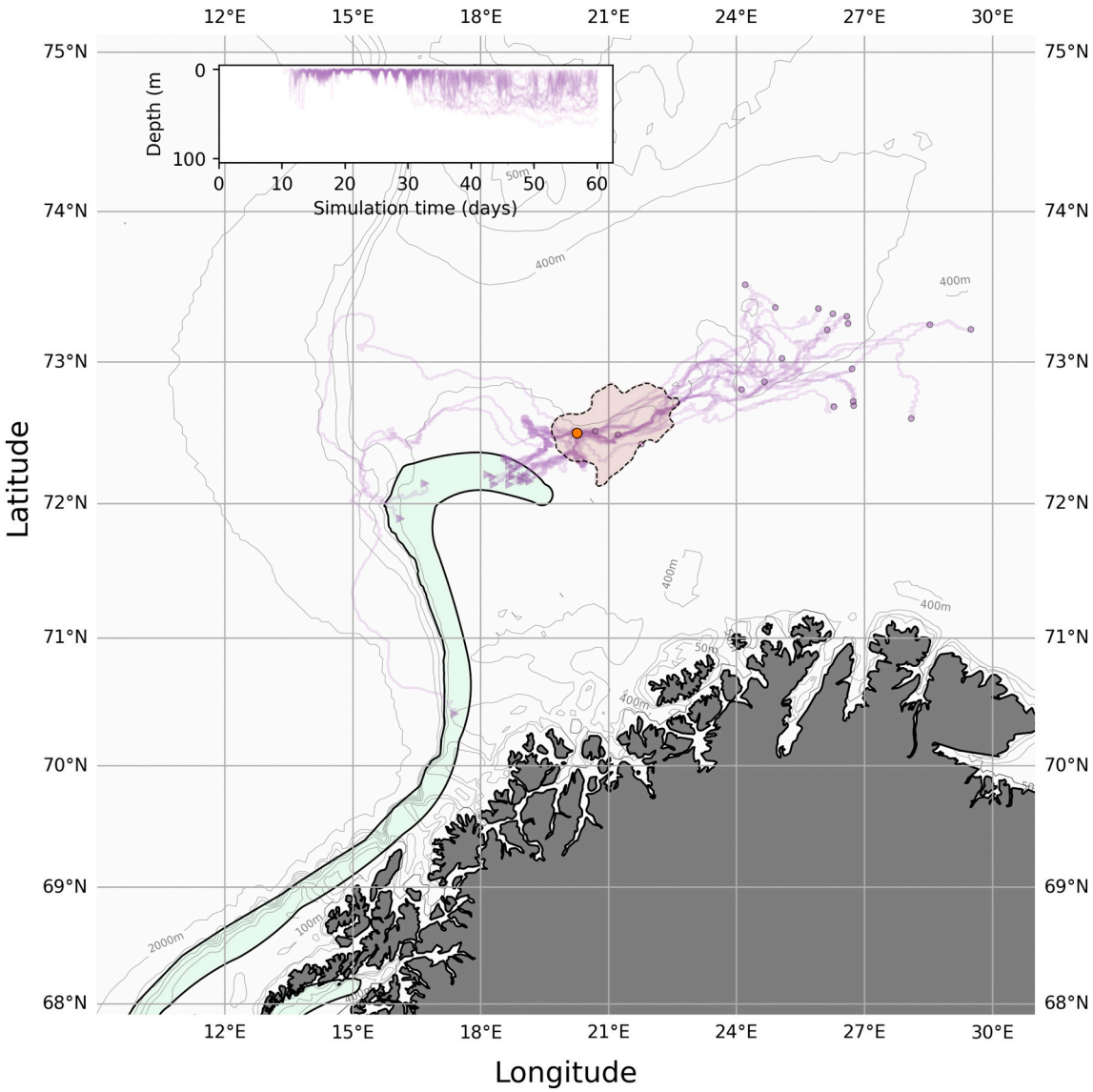

Fig. 6. Trajectories of the 20 super-individuals with the highest internal concentrations (purple tracks). The time- and depth-maximum total concentration of PW above 10 ng/L is indicated by the shaded light brown area. The insert in the upper left corner shows the depth position of the top 20 super-individuals over time. Note that the different development stages have different buoyancy properties in the model setup, leading to the eggs being located in the upper water column. (For interpretation of the references to color in this figure legend, the reader is referred to the web version of this article.)

List of abbreviations

ACR	Acute-to-chronic ratio
BTEX	Benzene, toluene, ethylbenzene, xylene
DNA	Deoxyribonucleic acid
DREAM	Dose-related Risk and Effects Assessment Model
ECHA	European Chemical Agency
EFSA	European Food Safety Authority
EIF	Environmental Impact Factor
ELS	Early life stages
ERA	Environmental risk assessment
GUTS	General Unified Threshold model of Survival
GUTS-IT	General Unified Threshold model of Survival (Individual Tolerance)
GUTS-SD	General Unified Threshold model of Survival (Stochastic Death)
IBM	Individual based model
IOGP	International Oil and Gas Producers
NCS	Norwegian Continental Shelf
NEC	No-effect concentration
OMEGA	Optimal Modeling for Ecotoxicological Applications
OSPAR	Oslo-Paris convention
PAH	Polyaromatic hydrocarbons
PEC	Predicted environmental concentrations
PNEC	Predicted no-effect concentration
PW	Produced water
QSAR	Quantitative Structure-Activity Relationship
RBA	Risk-based approach
ROMS	Regional Ocean Modeling System
TKTD	Toxicokinetic-toxicodynamic
WET	Whole effluent toxicity
WOA	World Ocean Atlas

CRediT authorship contribution statement

Raymond Nepstad: Conceptualization, Methodology, Software, Formal analysis, Investigation, Writing – original draft, Writing – review & editing, Visualization, Project administration, Funding acquisition.

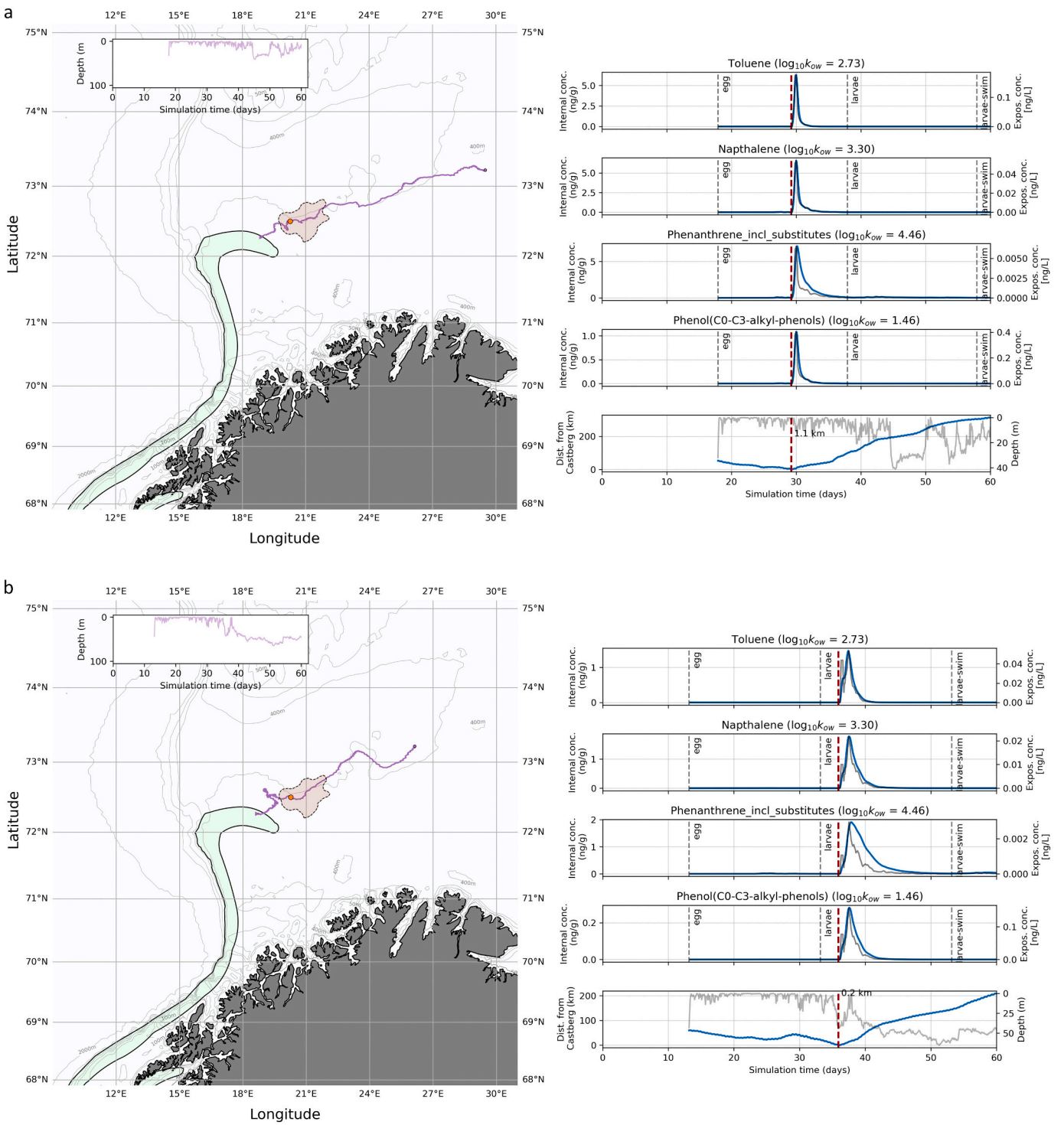

Fig. 7. Component internal concentration time series (blue full lines, right panels) and corresponding trajectory (left maps), for the super-individual with the highest total time-maximum internal concentration (top row) and 10th highest (lower row). External exposure concentrations are also shown (grey full lines, right axis of right panels). Distance of the super-individuals to Castberg is also shown in the lowermost panels on the right (full blue line, left axis), and depth (full grey line, right axis). The current stage for each super-individual is also indicated (egg, larvae, larvae-swim). In the maps, the time- and depth-maximum total concentration of PW above 10 ng/L is indicated (shaded light brown area). (For interpretation of the references to color in this figure legend, the reader is referred to the web version of this article.)

Konstantinos Kotzakoulakis: Methodology, Software, Investigation, Writing – original draft, Writing – review & editing. **Bjørn Henrik Hansen:** Conceptualization, Writing – original draft, Writing – review & editing. **Tor Nordam:** Conceptualization, Methodology, Writing – original draft, Writing – review & editing. **JoLynn Carroll:** Conceptualization, Writing – original draft, Writing – review & editing.

Declaration of competing interest

The authors declare that they have no known competing financial interests or personal relationships that could have appeared to influence the work reported in this paper.

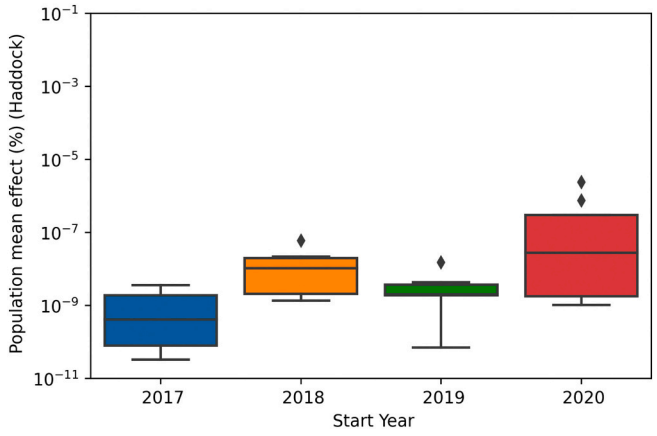

Fig. 8. Ensemble simulation summary results for the Castberg case (population-mean chronic mortality). The results have been grouped by simulation year, with different start dates within those years making up the variability in each box.

Data availability

The model is closed source, see www.sintef.no/DREAM.

Acknowledgements

This work was conducted under the Joint Industry Project *DREAM-MER Phase II*, funded by Aker BP, Equinor, NOROG, Total E&P Norge and Vår Energi. The authors would like to thank Trond Nordtug, Lars Petter Myhre and Tone Karin Frost for useful discussions, and for providing comments on the manuscript.

Appendix A. Supplementary material

Supplementary data to this article can be found online at https://doi.org/10.1016/j.marpolbul.2023.114979.

References

Adams, W.J., Blust, R., Borgmann, U., Brix, K.V., DeForest, D.K., Green, A.S., Meyer, J.S., McGeer, J.C., Paquin, P.R., Rainbow, P.S., Wood, C.M., 2011. Utility of tissue residues for predicting effects of metals on aquatic organisms. Integr. Environ. Assess. Manag. 7, 75–98.

Baas, J., Spurgeon, D., Broerse, M., 2015. A simple mechanistic model to interpret the effects of narcotics. SAR QSAR Environ. Res. 26, 165–180.

Bagi, A., Pampanin, D.M., Brakstad, O.G., Kommedal, R., 2013. Estimation of hydrocarbon biodegradation rates in marine environments: a critical review of the Q10 approach. Mar. Environ. Res. 89, 83–90.

Baird, W.M., Hooven, L.A., Mahadevan, B., 2005. Carcinogenic polycyclic aromatic hydrocarbon-dna adducts and mechanism of action. Environ. Mol. Mutagen. 45, 106–114.

Bart, S., Jager, T., Robinson, A., Lahive, E., Spurgeon, D.J., Ashauer, R., 2021. Predicting mixture effects over time with toxicokinetic-toxicodynamic models (GUTS): assumptions, experimental testing, and predictive power. Environ. Sci. Technol. 55, 2430–2439.

Beyer, J., Myhre, L.P., Sundt, R.C., Meier, S., Tollefsen, K.-E., Vabø, R., Klungsøyr, J., Sanni, S., 2012. Environmental risk assessment of alkylphenols from offshore produced water on fish reproduction. Mar. Environ. Res. 75, 2–9.

Beyer, J., Goksøyr, A., Hjermann, D.Ø., Klungsøyr, J., 2020. Environmental effects of offshore produced water discharges: a review focused on the Norwegian continental shelf. Mar. Environ. Res. 162, 105155.

Bogstad, B., Dingsør, G.E., Ingvaldsen, R.B., Gjøsæter, H., 2013. Changes in the relationship between sea temperature and recruitment of cod, haddock and herring in the barents sea. Mar. Biol. Res. 9, 895–907.

Brooks, S.J., Harman, C., Grung, M., Farmen, E., Ruus, A., Vingen, S., Godal, B.F., Baršienė, J., Andreikėnaitė, L., Skarphéinsdóttir, H., Liewenborg, B., Sundt, R.C., 2011. Water column monitoring of the biological effects of produced water from the ekofisk offshore oil installation from 2006 to 2009. J. Toxic. Environ. Health A 74, 582–604.

Carroll, J., Vikebø, F., Howell, D., Broch, O.J., Nepstad, R., Augustine, S., Skeie, G.M., Bast, R., Juselius, J., 2018. Assessing impacts of simulated oil spills on the northeast arctic cod fishery. Mar. Pollut. Bull. 126, 63–73.

Carroll, J., Frøysa, H.G., Vikebø, F., Broch, O.J., Howell, D., Nepstad, R., Augustine, S., Skeie, G.M., Bockwoldt, M., 2022. An annual profile of the impacts of simulated oil spills on the northeast arctic cod and haddock fisheries. Mar. Pollut. Bull. 184, 114207.

Cedergreen, N., Dalhoff, K., Li, D., Gottardi, M., Kretschmann, A.C., 2017. Can toxicokinetic and toxicodynamic modeling be used to understand and predict synergistic interactions between chemicals? Environ. Sci. Technol. 51, 14379–14389.

E. P. on Plant Protection Products, their Residues P.P.R.collab, Ockleford, C., Adriaanse, P., Berny, P., Brock, T., Duquesne, S., Grilli, S., Hernandez-Jerez, A.F., Bennekou, S.H., Klein, M., et al., 2018. Scientific opinion on the state of the art of toxicokinetic/toxicodynamic (tktd) effect models for regulatory risk assessment of pesticides for aquatic organisms. EFSA Journal 16, e05377.

Dahl-Hansen, I.E., Sagerup, K., Dahl-Hansen, G., Biuw, M., Falk-Petersen, S., Emblow, C., 2017. Virkninger for marint naturmiljø ved utbygging og drift av johan castberg. In: Technical Report 6397-04.

De Hoop, L., Huijbregts, M.J., Schipper, A.M., Veltman, K., De Laender, F., Viaene, K.P.J., Klok, C., Hendriks, J., 2013. Modelling bioaccumulation of oil constituents in aquatic species. Mar. Pollut. Bull. 76, 178–186.

De Vries, P., Jak, R.G., Frost, T.K., 2022. Comparison of substance-based and whole-effluent toxicity of produced water discharges from Norwegian offshore oil and gas installations. Environ. Toxicol. Chem. 41, 2285–2304.

Di Toro, D.M., McGrath, J.A., Stubblefield, W.A., 2007. Predicting the toxicity of neat and weathered crude oil: toxic potential and the toxicity of saturated mixtures. Environ. Toxicol. Chem. 26, 24–36.

Ditlevsen, M.K., 2017. Eif beregninger for produsert vann fra johan castberg 2016. In: Technical Report OC2017 F-047.

Durell, G., Utvik, T.R., Johnsen, S., Frost, T., Neff, J., 2006. Oil well produced water discharges to the north sea. Part i: comparison of deployed mussels (mytilus edulis), semi-permeable membrane devices, and the dream model predictions to estimate the dispersion of polycyclic aromatic hydrocarbons. Mar. Environ. Res. 62, 194–223.

ECHA, 2008. Guidance on information requirements and chemical safety assessment. In: Technical report, ECHA.

EU, 2003. Technical Guidance Document on Risk Assessment Part III. Technical Report.

French-McCay, D.P., 2002. Development and application of an oil toxicity and exposure model, oiltoxex. Environ. Toxicol. Chem. 21, 2080–2094.

Gauthier, P.T., Norwood, W.P., Prepas, E.E., Pyle, G.G., 2014. Metal–pah mixtures in the aquatic environment: a review of co-toxic mechanisms leading to more-than-additive outcomes. Aquat. Toxicol. 154, 253–269.

Gergs, A., Gabsi, F., Zenker, A., Preuss, T.G., 2016. Demographic toxicokinetic-toxicodynamic modeling of lethal effects. Environ. Sci. Technol. 50, 6017–6024.

Grimm, V., Railsback, S.F., 2005. Individual-based Modeling and Ecology. Princeton Universty Press, New Jersey.

Hendriks, A., van der Linde, A., Cornelissen, G., Sijm, D.T., 2001. The power of size. 1. Rate constants and equilibrium ratios for accumulation of organic substances related to octanol-water partition ratio and species weight. Environ. Toxicol. Chem. 20, 1399–1420.

Hiki, K., Iwasaki, Y., 2020. Can we reasonably predict chronic species sensitivity distributions from acute species sensitivity distributions? Environ. Sci. Technol. 54, 13131–13136.

Hylland, K., Tollefsen, K.-E., Ruus, A., Jonsson, G., Sundt, R.C., Sanni, S., Røe Utvik, T.I., Johnsen, S., Nilssen, I., Pinturier, L., Balk, L., Barien, J., Marigòmez, I., Feist, S.W., Børseth, J.F., 2008. Water column monitoring near oil installations in the north sea 20012004. Mar. Pollut. Bull. 56, 414–429.

IOGP, 2020. Risk Based Assessment of Offshore Produced Water Discharges. Technical Report. IOGP.

Jager, T., 2016. Predicting environmental risk: a road map for the future. J. Toxic. Environ. Health A 79, 572–584.

Jager, T., Ashauer, R., 2018. Modelling survival under chemical stress: A comprehensive guide to the GUTS framework.

Jager, T., Albert, C., Preuss, T.G., Ashauer, R., 2011. General unified threshold model of survival - a toxicokinetic-toxicodynamic framework for ecotoxicology. Environ. Sci. Technol. 45, 2529–2540.

Jager, T., Øverjordet, I.B., Nepstad, R., Hansen, B.H., 2017. Dynamic links between lipid storage, toxicokinetics and mortality in a marine copepod exposed to dimethylnaphthalene. Environ. Sci. Technol. 51, 7707–7713.

Johnsen, S., Frost, T., Hjelsvold, M., Utvik, T., 2000. The Environmental Impact Factor - a proposed tool for produced water impact reduction, management and regulation. In: SPE International Conference on Health, Safety and Environment in Oil and Gas Exploration and Production.

Karman, C.C., Smit, M.G., 2019. Whole effluent toxicity data and discharge volumes to assess the likelihood that environmental risks of offshore produced water discharges are adequately controlled. Integr. Environ. Assess. Manag. 15, 584–595.

Lee, K., Neff, J., 2011. Produced Water: Environmental Risks and Advances in Mitigation Technologies. Springer.

Lien, V.S., Gusdal, Y., Albretsen, J., Melsom, A., Vikebø, F.B., 2013. Evaluation of a Nordic Seas 4 km numerical ocean model hindcast archive (SVIM), 1960-2011. In: Technical Report 7. Havforskningsinstituttet.

Liubartseva, S., Federico, I., Coppini, G., Lecci, R., 2021. Stochastic oil spill modeling for environmental protection at the port of Taranto (southern Italy). Mar. Pollut. Bull. 171, 112744.

Locarnini, M., Mishonov, A., Baranova, O., Boyer, T., Zweng, M., Garcia, H., Seidov, D., Weathers, K., Paver, C., Smolyar, I., et al., 2018. World ocean atlas 2018. In: Temperature. Report, 1.

Lofthus, S., Almås, I.K., Evans, P., Pelz, O., Brakstad, O.G., 2018. Biodegradation in seawater of PAH and alkylphenols from produced water of a North Sea platform. Chemosphere 206, 465–473.
McCarty, L.S., Mackay, D., 1993. Enhancing ecotoxicological modeling and assessment. body residues and modes of toxic action. Environmental Science & Technology 27, 1718–1728.
McGrath, J.A., Di Toro, D.M., 2009. Validation of the target lipid model for toxicity assessment of residual petroleum constituents: monocyclic and polycyclic aromatic hydrocarbons. Environ. Toxicol. Chem. 28, 1130–1148.
Meador, J.P., Adams, W.J., Escher, B.I., McCarty, L.S., McElroy, A.E., Sappingtonyy, K. G., 2011. The tissue residue approach for toxicity assessment: findings and critical reviews from a society of environmental toxicology and chemistry pellston workshop. Integr. Environ. Assess. Manag. 7, 2–6.
Nepstad, R., Hansen, B.H., Skancke, J., 2021. North Sea produced water PAH exposure and uptake in early life stages of Atlantic cod. Mar. Environ. Res. 163, 105203.
Nepstad, R., Nordam, T., Ellingsen, I.H., Eisenhauer, L., Litzler, E., Kotzakoulakis, K., 2022. Impact of flow field resolution on produced water transport in lagrangian and eulerian models. Mar. Pollut. Bull. 182, 113928.
Nepstad, R., Skancke, J., Hansen, B.H., 2022. DREAM produced water plume and uptake simulations - predictions and comparisons with data from the 2021 water column monitoring at Ekofisk: plume trajectory and PAH uptake in mussels and copepods. In: Technical Report 2022:01303 A. SINTEF Ocean.
Niu, H., Lee, K., Robinson, B., Cobanli, S., Li, P., 2016. Monitoring and modeling the dispersion of produced water on the Scotian shelf. Environmental Systems Research 5, 19.
Nordam, T., Brönner, U., Daae, R.L., 2016. Convergence of ensemble simulations for environmental risk assessment. In: AMOP Technical Seminar on Environmental Contamination and Response-2008-2017. Environment and Climate Change Canada.
Nordam, T., Dunnebier, D.A., Beegle-Krause, C.J., Reed, M., Slagstad, D., 2017. Impact of climate change and seasonal trends on the fate of arctic oil spills. Ambio 46, 442–452.
North, E.W., Gallego, A., Petitgas, P., Ådlandsvik, B., Bartsch, J., Brickman, D., Browman, H.I., Edwards, K., Fiksen, Ø., Hermann, A.J., Hinckley, S., Houde, E., Huret, M., Lacroix, G., Leis, J.M., Mccloghrie, P., Megrey, B.A., Miller, T., Molen, J.V. D., Mullon, C., Parada, C., Paris, C.B., Pepin, P., Rose, K., Thygesen, U.H., Werner, C., 2009. Manual of recommended practices for modelling physical biological interactions during fish early life Editors. In: Technical Report.
Ospar, 2012. Guidelines in support of recommendation 2012/5 for a risk-based approach to the management of produced water discharges from offshore installations. OSPAR Commission.
OSPAR, 2014. Establishment of a list of predicted no effect concentrations (PNECs) for naturally occurring substances in produced water. In: Technical Report.
OSPAR, 2019. Discharges, spills and emissions from offshore oil and gas installations in 2017. In: Technical Report.
Reed, M., Hetland, B., 2002. DREAM: a dose-related exposure assessment model technical description of physical-chemical fates components. In: Proceedings of SPE International Conference on Health, Safety and Environment in Oil and Gas Exploration and Production. Society of Petroleum Engineers.
Reed, M., Rye, H., 2011. The DREAM model and the environmental impact factor: decision support for environmental risk management. In: Produced Water. Springer, pp. 189–203.
Rye, H., Reed, M., Ekrol, N., 1998. Sensitivity analysis and simulation of dispersed oil concentrations in the north sea with the provann model. Environ. Model Softw. 13, 421–429.
Sardi, A.E., Augustine, S., Olsen, G.H., Camus, L., 2019. Exploring inter-species sensitivity to a model hydrocarbon, 2-methylnaphtalene, using a process-based model. Environ. Sci. Pollut. Res. 26, 11355–11370.
Scheffer, M., Baveco, J.M., DeAngelis, D.L., Rose, K.A., van Nes, E.H., 1995. Super-individuals a simple solution for modelling large populations on an individual basis. Ecol. Model. 80, 161–170.
van Sebille, E., Griffies, S.M., Abernathey, R., Adams, T.P., Berloff, P., Biastoch, A., Blanke, B., Chassignet, E.P., Cheng, Y., Cotter, C.J., Deleersnijder, E., Döös, K., Drake, H.F., Drijfhout, S., Gary, S.F., Heemink, A.W., Kjellsson, J., Koszalka, I.M., Lange, M., Lique, C., MacGilchrist, G.A., Marsh, R., Adame, C.G.Mayorga, McAdam, R., Nencioli, F., Paris, C.B., Piggott, M.D., Polton, J.A., Rühs, S., Shah, S.H., Thomas, M.D., Wang, J., Wolfram, P.J., Zanna, L., Zika, J.D., 2018. Lagrangian ocean analysis: fundamentals and practices. Ocean Modelling 121, 49–75.
Smit, M.G.D., Frost, T.K., Johnsen, S., 2011. Achievements of risk-based produced water management on the Norwegian continental shelf (2002–2008). Integr. Environ. Assess. Manag. 7, 668–677.
World Meteorological Organization, 2012. Guidelines on ensemble prediction systems and forecasting. In: Technical Report. World Meteorological Organization.